Blocking ET-1 Receptors Does Not Correct Subnormal Retinal Oxygenation Response in Experimental Diabetic Retinopathy

Robin Roberts,[1] *Hongmei Luan,*[1] *and Bruce A. Berkowitz*[1,2]

PURPOSE. To test the hypothesis that bosentan (a dual ET_A/ET_B receptor antagonist) corrects a subnormal retinal oxygenation response in the STZ-induced diabetic rat.

METHODS. In benchtop experiments, ET-1 was acutely injected into the vitreous of control and 5- to 7-day bosentan-treated nondiabetic rats. Major retinal vessel diameters were analyzed from ADPase-stained flatmounts. Retinal oxygenation (ΔP_{O_2}), an established early surrogate marker of drug treatment efficacy, was measured by MRI during a 2-minute carbogen inhalation challenge in four groups: control rats ($n = 7$), control rats treated with bosentan ($n = 7$), 3-month diabetic rats ($n = 9$), and 3-month diabetic rats treated with bosentan ($n = 5$). Effect of baseline differences was studied in control rats breathing either room air ($n = 5$) or 12% oxygen breathing ($n = 5$) before a 2-minute carbogen provocation.

RESULTS. ET-1 produced a significant ($P < 0.05$) reduction in retinal arterial diameter that was suppressed ($P > 0.05$) in rats fed bosentan chow admix. For all groups, no MRI baseline signal intensity differences were found ($P > 0.05$). Also, comparisons between baseline room air and 12% conditions and control rats fed normal chow or a bosentan admix both produced similar ($P > 0.05$) panretinal ΔP_{O_2}. In treated and untreated diabetes groups, inferior hemiretinal ΔP_{O_2} remained normal ($P > 0.05$), but superior hemiretinal ΔP_{O_2} was subnormal ($P < 0.05$).

CONCLUSIONS. Because subnormal retinal ΔP_{O_2} after drug treatment is a biomarker of subsequent vascular histopathology, the present data raise the possibility that retinal ET-1 does not play a key role in the pathogenesis of diabetic retinopathy. (*Invest Ophthalmol Vis Sci.* 2006;47:3550–3555) DOI:10.1167/iovs.05-1624

The abnormal biochemistry underlying diabetes-induced retinal hemodynamic pathophysiology is not well understood. Increased retinal expression of endothelin (ET) is thought to contribute to the reduction of retinal blood flow reported in the early stages of diabetes mellitus.[1–3] ET is a 21-amino-acid peptide that is found in three isoforms (ET-1, ET-2, ET-3), is released by endothelial cells and is a potent and long-lasting vasoconstrictor. Only ET-1 and ET-3 are found in mammals. ET activity is regulated by two ET receptors: ET_A and ET_B. The ET_A receptor has the greatest affinity for ET-1 and the ET_B receptor shows equal affinity for all three isoforms. The ET_A receptor appears primarily to mediate vasoconstriction, whereas the ET_B receptor can mediate both vasoconstriction and vasodilatation. Normally, increased ET levels are primarily responsible for retinal vessel constriction during 100% oxygen breathing in humans and in rats.[4] The role of retinal ET in diabetes-induced alternations of retinal oxygenation is not yet known.

The retinal oxygenation response to a hyperoxic provocation (ΔP_{O_2}), measured by functional MRI, is a powerful and noninvasive biomarker of the retinovascular system's ability to oxygenate, has been validated as a useful and early surrogate for assessing drug treatment efficacy in experimental diabetic retinopathy, and is clinically applicable.[5] We, and others, have shown in animal models that retinal ΔP_{O_2} during a carbogen (a gas mixture of carbon dioxide [5% CO_2] and oxygen [95% O_2]) inhalation challenge generates maximal ΔP_{O_2}, compared with 100% oxygen breathing.[5–7] In Sprague-Dawley rats, ΔP_{O_2} is significantly lower than normal (i.e., subnormal) in experimental diabetes before the appearance of retinal histopathology.[5] In addition, we have found that drug treatments which prevent the appearance of retinal structural lesions also correct the early development of reduced retinal oxygenation response. Drugs that did not prevent diabetes-related vascular histopathology, did not correct the early subnormal ΔP_{O_2}.[5] The biochemical basis regulating the appearance of diabetic retinopathy or a subnormal retinal ΔP_{O_2} is not well understood.

Previous studies have suggested that there may be a relationship between elevated ET-1, diabetic retinopathy, and subnormal retinal ΔP_{O_2}. For example, an acute injection of ET-1 into the vitreous of nondiabetic control animals produced an initial subnormal ΔP_{O_2}, compared with vehicle-injected vitreous.[5] Also, in diabetic rats, the beneficial effects of aminoguanidine (AMG) on the initial ΔP_{O_2} after 3 months of diabetes may be related to reduced ET-1 expression by the inhibitory effect of AMG on the activity of protein kinase C (PKC).[8,9] PKC activity is increased in the diabetic rat retina, and PKC is a known modulator of ET expression.[10] However, AMG is an antioxidant and corrects other biochemical abnormalities associated with diabetes, such as increased inducible nitric oxide synthase.[8,11] Together, these considerations suggest, but do not prove, that ET-1, acting through its receptors, plays an important role in altering the temporal evolution of retinal ΔP_{O_2} in diabetes.

In this study, we tested the hypothesis that bosentan (a dual ET_A/ET_B receptor antagonist) can be used to treat diabetic retinopathy in the STZ-induced diabetic rat. Bosentan is a dual ET_A/ET_B receptor antagonist that is reported to be well tolerated and effective after 5 months of oral treatment in control and diabetic rats without overt side effects such as increased blood pressure.[12–15] Furthermore, bosentan treatment has been reported to correct diabetes-induced increases in retinal ET-1 mRNA expression, retinal fibronectin, NF-κB, activating protein (AP) activation, and basement membrane thickening.[16] The dose 100 mg/kg bosentan administered orally has been well established in the rat as being adequate for competitively antagonizing the ET receptor system over long periods.[14,15,17,18]

Methods

The animals were treated in accordance with the NIH Guide for the Care and Use of Laboratory Animals and the ARVO Statement for the Use of Animals in Ophthalmic and Vision Research.

Benchtop Experiments

In the benchtop study, intravitreal injections of ET-1 (10^{-5} or 10^{-6} M in 1 μL bolus delivered intravitreally through a 10 μL Hamilton syringe) or vehicle (2.5% emulphor in phosphate-buffered saline; kindly provided by Allen Clermont, Beetham Eye Institute, Joslin Diabetes Center, Boston, MA) were performed in control rats fed rat either normal chow or chow admixed with 100 mg/kg bosentan (kind gift of Actelion, Allschwil/Basel, Switzerland) orally for 5 to 7 days. Untreated rats were fed normal rat chow (5001; Ralston Purina, Richmond, IN) and water ad libitum. For treated rats, the diet was supplemented with either 1500 or 600 mg bosentan/kg food. Assuming that the food consumption of a 250-g control rat is ~16 g/d, the average amount of bosentan consumed in the two treatment groups was ~100 mg/kg body weight (BW)/d and 40 mg/kg BW/d, respectively.

Vessel Diameters

Ten minutes after ET-1 injection, the eyes were enucleated, flat-mounted, and stained with adenosine diphosphatase (ADPase), as previously described.[19,20] Retinal vessel diameters were determined from images of these flatmounts captured by a CCD camera with a fixed focus, lens, and magnification, and analyzed on computer (Power Mac G4; Apple Computer, Cupertino, CA) with the program NIH Image (available by ftp at zippy.nimh.nih.gov/ or at http://rsb.info.nih.gov/nih-image; developed by Wayne Rasband, National Institutes of Health, Bethesda, MD). The measurement system was spatially calibrated with a ruler before each set of measurements. The diameters of all major vessels were measured from a fixed distance (1 mm) from the optic nerve head. In untreated control rats, the median vessel diameter was 35.75 μm ($n = 9$). We interpreted diameters above and below this median as strongly weighted toward vein and artery values, respectively. This assumption was confirmed by detecting the expected effects of acute ET-1 injections on arteries and veins (Fig. 1).[21,22]

Animal Groups for the MRI Experiments

In the baseline–MRI study, control rats started at different baselines (room air [RA] or 12% oxygen breathing [12%]) followed by a 2-minute carbogen provocation. In the ET-1–MRI study, rats were randomized into four groups. The groups were: nondiabetic age-matched control

Figure 1. Summary of vessel diameters that are either venous (i.e., >35.75 μm, *left*) or arterial (i.e., <35.75 μm, *right*) weighted. The numbers of animals used to generate these data are listed above each bar. Error bars, SEM. *$P < 0.05$ was significant.

subjects (C), nondiabetic age-matched control animals treated orally with bosentan for 2 weeks (C+B), untreated diabetic rats 3 months after the initiation of hyperglycemia (D), and diabetic rats treated orally for 3 months with bosentan (D+B). No intraocular ET-1 injections were performed in any of the groups studied by MRI. Oral treatment consisted of a diet for the control and diabetic rats supplemented with either 1500 mg bosentan/kg food or 600 mg bosentan/Kg food, respectively. Diabetic rats consume approximately 2.5 times more chow than do control subjects (Kern T, Kowluru R, personal communications, 2003). This yielded an estimated dose of bosentan consumed per day in each group as 100 mg/kg BW. According to the company, bosentan is stable at room temperature and is not light sensitive in the solid form. Thus, the diet is not expected to have lost biopotency at any point during this study. Nonetheless, the admixed diet was stored sealed in a darkroom that had the heater vent turned off. Chow was kept under these conditions for 1 to 2 months before the rats began the diet.

Diabetes was induced with an intraperitoneal injection of streptozotocin (60 mg/kg) within 5 minutes of its preparation in 0.01 M citrate buffer (pH 4.5) in rats, with a body weight of approximately 200g after an overnight fast. Diabetes was verified 3 days later by the presence of plasma hyperglycemia ($\geq$200 mg/dL) and elevated urine volume (>60 mL/d) in nonfasted rats. Rat body weight, average food consumption, and blood glucose levels were monitored weekly. Subtherapeutic levels of insulin (0–2 U of neutral protamine Hagedorn [NPH] insulin administered subcutaneously daily) were administered to maintain blood glucose levels between 450 and 550 mg/dL without urine ketones (see Table 1). Glycated hemoglobin (GHb) was measured after 2 months of diabetes using affinity columns (Glyco-Tek kit 5351; Helena Laboratories, Beaumont, TX).

MRI Examination

On the day of the experiment, blood glucose level was measured before anesthesia in each animal by tail nick. Anesthesia was then induced by a single intraperitoneal injection of urethane (36% solution, 0.083 mL/20 g animal weight, prepared fresh daily; Aldrich, Milwaukee, WI). Each animal was gently positioned on an MRI-compatible homemade holder with its nose placed in a plastic nose cone. Animals were allowed to breathe spontaneously during the experiment. To maintain the core temperature, a recirculating heated water blanket was used. Rectal temperature was continuously monitored, while the animal was inside the magnet, as previously described.[9]

MRI data were acquired in a manner similar to that previously described on a 4.7-T system using a two-turn transmit/receive surface coil (1.0 cm diameter) placed over the eye. Images were acquired by using an adiabatic spin-echo imaging sequence (repetition time TR 1 second, echo time TE 22.7 ms (the shortest echo time allowed with this sequence), number of acquisitions NA 1, matrix size 128 × 256, slice thickness 1 mm, field of view 32 × 32 mm^2, sweep width 25,000 Hz, 2 minutes/image).[23] This method resulted in an in-plane resolution of 250 × 125 μm^2. Sagittal localizer images were first collected and used to position a single 1-mm transverse slice through the center of the eye. The 1-mm slice thickness was needed to obtain an adequate signal-to-noise ratio in a 2-minute image. This slice thickness resulted in some partial volume averaging so that the final image contained superior and inferior hemiretina with some relatively minor contribution from the temporal and nasal hemiretina. It is important to note that steady state (room air) vitreous oxygen tension *cannot* be measured by using this method, because many factors affect the preretinal vitreous water signal and its relaxation properties. In other words, simply obtaining an image of the eye during room air breathing alone cannot be used to measure retinal oxygenation.

Bosentan/MRI data were collected as follows: three images while the animal breathed room air, and one image during the inhalation of carbogen. Carbogen inhalation was started at the end of the third image. Animals were returned to room air for 5 minutes to allow recovery from the inhalation challenge and were removed from the magnet. For the baseline–MRI study, data were collected as follows: three images while the animal breathed room air, four images while the
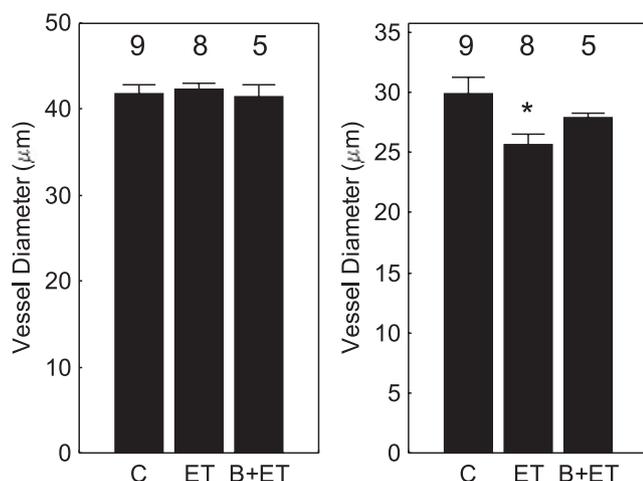
rat inhaled 12% oxygen, and one image collected during the inhalation of carbogen. Inhalation of 12% oxygen and carbogen was started at the end of the third or seventh images, respectively. In all cases, animals were returned to room air for 5 minutes, to allow recovery from the inhalation challenge and were removed from the magnet.

A second 2-minute carbogen challenge was performed outside the magnet with care taken to not alter the spatial relationship between the animal head and nose cone. At exactly 2 minutes, arterial blood from the descending abdominal aorta was collected, as described previously.[23] This blood was analyzed for P_aO_2, P_aCO_2, and pH. Note that this second inhalation challenge (outside the magnet) is needed because it is not feasible to routinely obtain an arterial blood sample from inside the magnet (>40 cm away from the magnet opening) from rats. In all cases, after the blood collection, animals were euthanized with an intracardiac potassium chloride injection. In addition, blood gas readings were also obtained as in the benchtop experiments in control rats breathing either room air ($n = 4$) or 12% oxygen ($n = 5$).

Data Analysis

To be included in the MRI portion of the study, the animal had to demonstrate (1) minimal eye movement during the MRI examination. Movement artifacts (typically seen in the phase encode direction) confound interpretation of the vitreous signal intensity changes produced during the hyperoxic challenge; (2) nongasping respiratory pattern before and after the MRI examination. If the animal is gasping (which occurred $<1\%$ of the time), the anesthetic was probably inadvertently administered into an organ. This could produce a change in systemic oxygenation unrelated to the retinal changes; (3) rectal temperatures in the range of 35.5 °C to 36.5°C. Preliminary experiments (data not shown) found a strong association between core temperature and P_aCO_2 and P_aO_2 levels. The effect of this correlation on the precision of the measurements was minimized by using a relatively tight range of temperatures; (4) $P_aO_2 >350$ mm Hg and P_aCO_2 between 46 and 65 mm Hg during the carbogen challenge. Previously, we found that arterial oxygen levels above 350 mm Hg during a hyperoxic challenge were needed to produce a consistently large preretinal vitreous oxygenation response.[24,25] The range of acceptable arterial carbon dioxide levels lay within the array of values in the literature measured under carbogen breathing conditions. In addition, tight control over the acceptable blood gas range is needed to ensure adequate quality control of each sample. Occasionally, the blood gas machine was not able to read a sample (due to, e.g., a clot or excessive air in the capillary tube). In this case, the MRI data were also excluded. In general, ΔP_{O_2} data were collected approximately 60 minutes after urethane injection, to avoid potential errors due to variable time under anesthesia. The above acceptance criteria are needed to compare the retinal oxygenation response critically in these spontaneously breathing normal and sick animals while minimizing systemic differences. Because of these acceptance criteria, only approximately 50% to 80% of the animals that started the study were included in the final analysis. Although a relatively small number of animals are used for comparison, note that all the pixel values over a set retinal region are used in the comparison. For example, for the comparison of superior hemiretina 3 mm from the optic nerve, 24 pixels per rat are used for the seven rats in the control group and eight rats in the diabetic group. Thus, 168 and 192 pixel values, respectively, are being compared. Power calculations assume the acquisition of uncorrelated data. However, the pixels are spatially correlated. Thus, a power calculation is not appropriate. Instead, we took advantage of the fact that the generalized estimating equation approach fits the correlation structure between pixels. For this reason, and in our experience during the past 10 years, we found that a group size of five or more rats is adequate to determine statistical significance at the 95% confidence level.

To correct for any movement in the slice plane, a warp affine image co-registration was performed on each animal by using software written in-house. This procedure was used in all the animals included in the final analysis but was only necessary in approximately half of them, regardless of group (e.g., subtle shifting of the animals' position oc-

curred during the experiment due to settling on the gauze packing). We insured that the selected slice was the same one used throughout the series by carefully checking for differences in the size of lens and optic nerve in each image. In addition, because the slice thickness (1 mm) is relatively large compared to the diameter of the eye (approximately 6 mm), partial volumes will be similar if the eye subtly moves out of the imaging plane and so the data analysis results are not expected to be substantially affected. After co-registration, the MRI data were transferred to the computer (Power Mac G4; Apple Computer) and analyzed with NIH Image. Images obtained during room air breathing were averaged to improve the signal-to-noise ratio. Signal intensity changes during carbogen breathing were calculated and converted to ΔP_{O_2} values, on a pixel-by-pixel basis, as follows.[23] For each pixel, the fractional signal enhancement, E, was calculated:

$$E = (S(t) - S_0)/S_0, \qquad (1)$$

where $S(t)$ is the pixel signal intensity at time t after starting the gas inhalation and S_0 is the control signal intensity (measured from the average of the three images obtained during room air breathing) at the same pixel spatial location. E values were converted into ΔP_{O_2} using theory that has been validated in the rat[26]:

$$\Delta P_{O_2} = E/(R_1 \cdot T_k), \qquad (2)$$

where R_1 is the oxygen relaxivity (seconds$^{-1} \cdot$ mm Hg^{-1}), and $T_k = T_r \cdot \exp(-T_r/T_{10})$, T_r is the repetition time, and T_{10} is the T_1 in the absence of oxygen. Using a T_r of 1 second, and assuming a vitreous T_{10} of 4 seconds, $T_k = 3.52$. This T_{10} is based on our previous measurement of the proton spin-lattice relaxation time in the rabbit vitreous (4 seconds) and reported values in human vitreous (3.3 seconds) and cerebral spinal fluid (4.3 seconds), which has a high water content, similar to that of vitreous.[23,27–29] An R_1 of 2×10^{-4} s$^{-1} \cdot$ mm Hg^{-1} was used. This R_1 was previously measured in a saline phantom, which is assumed to be a reasonable model of vitreous (98% water).[23] A similar R_1 was found for plasma, suggesting that relatively low protein levels do not substantially contribute to the oxygen relaxivity.[30] Note that an E of 0.01 (i.e., a 1% signal intensity change) corresponds to a ΔP_{O_2} of 14 mm Hg. There did not appear to be any significant changes in vitreous T_{10} or R_1 in the animals of this study (data not shown).

The images were analyzed as follows. First, from either regular images or enhancement images, the pixel values along a 1-pixel-thick line drawn at the boundary of the retina and vitreous were set to 255 (black). We estimate that the thickness of this line, based on the in-plane resolution is approximately 100 μm. The values in another 1-pixel-thick line drawn in the preretinal vitreous next to the black pixels were then extracted.[19] This procedure minimized retinal–choroid pixel values from potentially contaminating ("pixel bleed") those used in the final analysis and insured that similar preretinal vitreous space was sampled for each animal. In addition, spatial averaging over these 100-μm regions of interest tend to minimize the contribution from the very local preretinal oxygenation gradients next to the retinal surface.[31] In addition, an average ΔP_{O_2} band was constructed based on the within-group mean for each pixel.

Statistical Analysis

All data are presented as the mean ± SEM, unless otherwise noted. The blood vessel diameter data and physiological parameters (i.e., blood gas values, rectal temperatures, blood glucose data) were normally distributed. Comparisons were performed using a one-way ANOVA or an unpaired 2-tailed t-test (unless otherwise noted). $P \leq 0.05$ was considered significant.

Comparison of retinal ΔP_{O_2} between control and experimental groups at each time point were performed using a generalized estimating equation approach,[32] which performs a general linear regression analysis using all the pixels in each subject and accounts for the within-subject correlation between adjacent pixels. Results from the literature are consistent with our present finding of a subnormal retinal

TABLE 1. Summary of Animal Model and Physiology (mean $\pm$ SEM)

	Weight (g)	GHb (%)	P_aco_2 (mm Hg)	P_ao_2 (mm Hg)	pH	Temp. (°C)
Supporting experiments						
C (room air)	280.0 $\pm$ 2.2	—	43 $\pm$ 2	100 $\pm$ 3	7.40 $\pm$ 0.02	36.9 $\pm$ 0.1
C (12%)	228.0 $\pm$ 1.8	—	40 $\pm$ 4	54 $\pm$ 2*	7.38 $\pm$ 0.03	36.5 $\pm$ 0.5
C (carbogen)	231.1 $\pm$ 6.6	—	55 $\pm$ 2*	535 $\pm$ 33*	7.27 $\pm$ 0.01*	36.7 $\pm$ 0.3
C+B (carbogen)	251.4 $\pm$ 10.5	—	58 $\pm$ 1*	555 $\pm$ 24*	7.29 $\pm$ 0.01*	36.1 $\pm$ 0.2
Main experiments						
C (carbogen)	288.7 $\pm$ 14.2	4.0 $\pm$ 0.1	51 $\pm$ 1	566 $\pm$ 22	7.31 $\pm$ 0.02	36.3 $\pm$ 0.2
D (carbogen)	267.6 $\pm$ 5.2	12.5 $\pm$ 0.9*	55 $\pm$ 1	495 $\pm$ 32	7.30 $\pm$ 0.02	36.8 $\pm$ 0.2
D+Bos (carbogen)	275.8 $\pm$ 3.8	14.0 $\pm$ 0.8*	59 $\pm$ 2*	524 $\pm$ 46	7.29 $\pm$ 0.02	36.4 $\pm$ 0.2

Data are the mean $\pm$ SEM.
* $P < 0.05$, compared with respective control group.

ΔPo_2 in the diabetic groups, supporting the lack of spurious significant findings.[5]

RESULTS

Vessel Diameters

In separate preliminary studies, we found no difference in retinal vessel diameters between untreated and vehicle-treated control rats (data not shown). Compared with control arterial weighted vessel diameters (29.95 $\pm$ 1.27 μm, $n = 9$), acute intravitreal injections of 10^{-5} and 10^{-6} M ET-1 produced diameters of 25.60 $\pm$ 0.99 μm ($n = 8$; 14.5% decrease, $P = 0.018$), and 28.65 $\pm$ 0.55 μm, $n = 4$ (4.3% decrease, $P = 0.37$), respectively. In contrast, arterial weighted vessel diameters in bosentan-treated rats after an intravitreal 10^{-5} M ET-1 injection were not different from control values (1500 mg/kg bosentan dose: 27.94 $\pm$ 0.34 μm, $n = 5$, $P = 0.16$; and 600 mg/kg bosentan dose: 28.12 $\pm$ 0.84 μm, $n = 7$, $P = 0.25$). The 1500-mg/kg dose results are summarized in Figure 1. No effect ($P > 0.05$) of ET-1 was found on venous-weight vessel diameter in any experimental group (Fig. 1).

Magnetic Resonance Imaging

Systemic Physiology. Summaries of systemic physiology are presented in Table 1. As expected, compared with control rats, all diabetic animals had significantly ($P < 0.05$) elevated glycated hemoglobin's (GHb) A summary of the blood parameters measured during a 2-minute carbogen challenge and core temperature during the experiment are also presented in Table 1. No significant differences ($P > 0.05$) were observed between any of the groups. Note that the blood gas values in all groups are within the expected range.[23] In addition, baseline blood gas values during 12% oxygen breathing revealed the expected decrease in arterial oxygen levels compared with room air breathing (Table 1).

Retinal Oxygenation Response. Comparison of baseline panpreretinal signal intensities revealed no significant ($P > 0.05$) differences between room air breathing (106.5 $\pm$ 0.9 AU) and 12% oxygen inhalation (107.0 $\pm$ 0.9 AU) or between the control group (113.7 $\pm$ 0.8 AU) and the two diabetic groups (114.0 $\pm$ 0.7 and 116.8 $\pm$ 0.7 AU, respectively).

Inhalation of 12% Oxygen. In control rats, retinal ΔPo_2 generated in room air conditions or 12% oxygen and a 2-minute carbogen challenge were not significantly ($P > 0.05$) different (Fig. 2).

Bosentan Treatment. Neither superior nor inferior hemiretinal ΔPo_2 from control rats fed normal chow (142 $\pm$ 6 and 147 $\pm$ 6 mm Hg, respectively) or a bosentan chow admix (113 $\pm$ 7 and 139 $\pm$ 7 mm Hg, respectively) were significantly ($P > 0.05$) different.

Diabetes. Figure 3 represents a summary of retinal ΔPo_2 during the first 2-minute carbogen provocation (i.e., t1-ra). Both experimental groups had similar inferior hemiretina ΔPo_2s compared with control subjects ($P = 0.32$ and 0.74, respectively) but subnormal superior hemiretina ΔPo_2s ($P = 0.04$ [one-tailed t-test] and 0.01, respectively). Note that retinal ΔPo_2 (2 minutes) measured in the two control groups in this work and summarized in Figures 2 and 3 are not significantly different ($P > 0.05$).

DISCUSSION

In this study, two major findings are reported: that early subnormal superior hemiretinal ΔPo_2 found in diabetic rats does not appear to depend on baseline conditions, and that treatment with a dual ET receptor antagonist did not correct subnormal superior oxygenation response, a biomarker of drug efficacy in the treatment of diabetic retinal vascular histopathology. Retinal mRNA expression of ET-1 has been reported to be significantly increased during the first 6 months of experimental diabetes in rats.[2,16] Furthermore, reductions in retinal perfusion observed by 1 month of diabetes could be corrected by endothelin receptor antagonists.[1,2] These results suggested a link between increased retinal ET-1 and reduced retinal perfusion. However, by 3 months (Chakrabarti S, personal com-
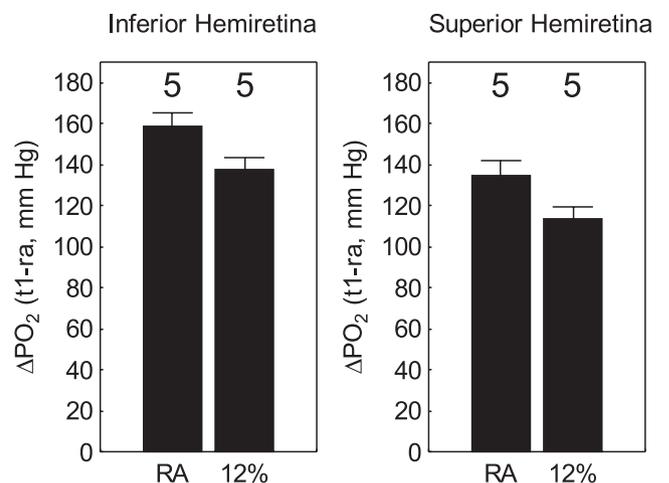

FIGURE 2. Summary of inferior (*left*) or superior (*right*) hemiretinal ΔPo_2 measured in control rats during the first 2 minutes on carbogen (i.e., t1-ra) from either room air (ra) or 12% oxygen breathing (12% baseline conditions). The numbers of animals used to generate these data are listed above each bar. Error bars, SEM. *$P < 0.05$ was significant.
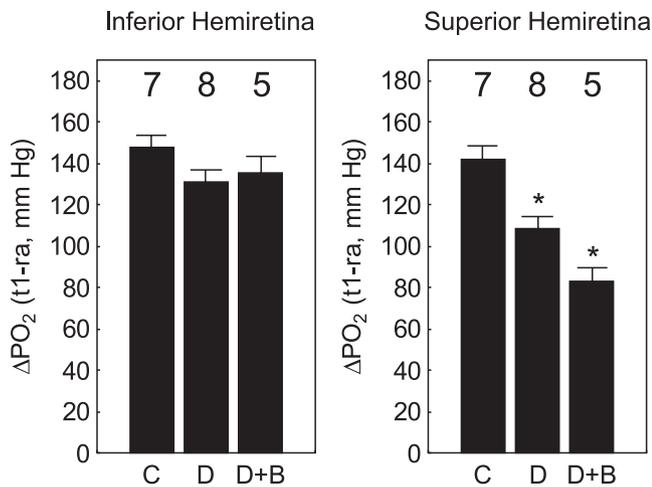
Inferior Hemiretina   Superior Hemiretina

FIGURE 3. Summary of inferior (*left*) or superior (*right*) hemiretinal ΔPO_2 measured during the first 2 minutes on carbogen (i.e., t1-ra). The numbers of animals used to generate these data are listed above each bar. Error bars, SEM. *$P < 0.05$ was significant.

munication, 2004) and 6 months of diabetes at least some of these hemodynamic abnormalities were no longer present.[1] Thus, the impact of increased altered expression of retinal ET-1 on diabetic retinovascular pathophysiology has been unclear and was investigated in this study.

Previous work involving bosentan and diabetic retinopathy have been done by the Chakrabarti group using the same dose and route (oral) as in the present study. These studies demonstrated that bosentan was effective at correcting diabetes-related basement membrane thickening, increased retinal fibronectin expression, activation of NF-$\kappa\beta$ and AP-1, and the 1-month reduction in retinal perfusion.[1,16,17,33,34] One difference is that we administered bosentan admixed with the chow while Chakrabarti et al. administered it via daily gavage.[17] In this study, we were able to confirm in separate benchtop experiments, that different doses of bosentan in a chow admixture effectively suppressed the vasoconstriction associated with an acute ET-1 challenge in control rats. It is not possible to determine the relevance of the conditions to that in diabetic rats, because the concentration of ET-1 in the vitreous or retina in diabetic rats is not currently known (Chakrabarti S, private communication, 2005). We suspect that the 10^{-5} M dose is too high to represent the actual concentration in vivo. However, this dose of ET-1 produced a relatively larger retinal arterial vasoconstriction making any subtle corrections produced by bosentan supplementation easier to detect statistically. In addition, we found that lowering the dose to 40 mg/kg BW/d did not significantly alter bosentan's effectiveness in correcting the arterial weighted vasoconstriction during an ET-1 challenge. In any event, the dose and route of the bosentan admixture used for the MRI experiments appears to be reasonable for addressing our hypothesis.

In this study, we also evaluated in control rats whether or not the combination of the 5% CO_2 in the gas challenge (which is expected to suppress vasoconstriction due to pure oxygen breathing) and bosentan (which is also expected to suppress vasoconstriction due to pure oxygen breathing) would increase superior and/or inferior hemiretinal ΔPO_2 relative to that from control rats breathing only carbogen. Neither superior nor inferior hemiretinal ΔPO_2 for control rats fed a bosentan admix diet for 2 weeks demonstrated a significant increase relative to control rats fed normal chow. In addition, no effect of the bosentan treatment was noted on inferior hemiretinal ΔPO_2 of control, untreated diabetic, or diabetic rats fed bosentan. Thus, it does not appear that the combination of bosentan

feeding and carbogen inhalation confounded interpretation of the MRI data.

Because of the negative result in this study, it was important to consider the possibility that the results were secondary to inadequate inhibition by bosentan. We were unable to directly evaluate the bioactivity of bosentan in the plasma of treated diabetic rats. However, we felt that a reasonable alternative was to measure the effectiveness of bosentan treatment in preventing vasoconstriction produced by intravitreally injected ET-1 in benchtop experiments. Throughout the course of these experiments, three separately constituted bosentan admix chows were evaluated. The first bosentan admix chow was used for the MRI experiments. We confirmed with Purina that the chow admix was properly constituted. After performing the MRI experiments, we then checked the potency of this chow admixture. Several control rats were fed this first bosentan chow admix for 1 week before their retinal vessels were inspected by operating microscope by two of the investigators (BAB, RR), before and after either control or ET-1 injection. We were able to confirm visually that the bosentan admix chow was effective at suppressing ET-1-induced retinal vessel vasoconstriction; unfortunately, the results of these experiments were not quantitatively documented. Subsequently, two more batches of bosentan chow were ordered and similarly evaluated on the benchtop. The data from these two experiments are presented in the manuscript and clearly demonstrate that different doses of bosentan mixed into the chow can effectively suppress vasoconstriction produced by greater than normal vitreous ET-1 levels. Taken together, these considerations support both the present use of bosentan as an adequate antagonist for addressing our hypothesis and the conclusion that the reported increase in retinal ET-1 with diabetes does not appear to play a key role in retinovascular dysfunction associated with 3 months of diabetes.

The mechanisms regulating retinal oxygenation responses to a carbogen provocation in normal and diabetic rats have yet to be completely worked out. In the present study, we did not measure baseline parameters, such as retinal vessel diameters, blood flow, or oximetry, that might affect the final ΔPO_2. It was not clear that such a difference would affect the results of the present study, since examination of the pan-preretinal vitreous baseline signal intensities did not reveal any differences between control and diabetic rats. This suggested that whatever baseline differences might have been present were not detectable on MRI. To investigate further a possible cause of the baseline difference, we examined the effect of a baseline hypoxemia condition before the carbogen provocation. Hypoxemia is well known for inducing a range of changes in retinal vessel diameter, blood flow, and oximetry, among other changes.[35-37] Even under this somewhat severe condition (12% oxygen), the 2-minute carbogen ΔPO_2 remained normal (Fig. 2). Taken together, these data suggest that baseline differences per se are either not responsible or not practically important (i.e., have no detectable impact) with regard to early subnormal superior hemiretinal ΔPO_2 found in diabetic rats.

In this study, we found the expected subnormal superior hemiretinal ΔPO_2 during a 2-minute carbogen inhalation in 3-month diabetic rats. This subnormal response is consistent with findings in five previous studies in experimentally diabetic rodents.[5] Thus, the hypothesis tested was that untreated diabetic rats in this study would have a superior hemiretina with a subnormal oxygenation response, and so a one-tailed result was used.

Retinal ΔPO_2, a measure of the health of the retinovascular system's regulatory response, has been established as an early predictor of therapeutic efficacy in experimental diabetes.[5,9,38] For example, drug treatment, such as AMG, that corrects the subnormal ΔPO_2 in 3-month diabetic rats, also corrects late-stage retinal histopathology.[5] Furthermore, treatments that do

not normalize this subnormal ΔP_{O_2} in 3-month diabetic rats do not prevent the development of histopathology.[5] In contrast, there is little consistent and direct evidence in the literature that steady state parameters, such as blood flow or oximetry, are linked with progression of diabetic retinopathy or its treatment response.[5,39] One reason for this may be that normally the retinovascular system is never at steady state and must constantly adapt. A dynamic mismatch can have long-term negative consequences for the health of the retina. Dynamic measures of the health of the retinovascular system may thus be a more relevant parameter for assessing drug treatment effects. Given this prognostic ability of MRI ΔP_{O_2}, the present results also raise the possibility that early changes in retinal ET-1 expression do not play an important role in the later development of diabetic retinopathy.

Acknowledgments

References

1. Deng D, Evans T, Mukherjee K, Downey D, Chakrabarti S. Diabetes-induced vascular dysfunction in the retina: role of endothelins. *Diabetologia.* 199942:1228–1234.

2. Takagi C, Bursell SE, Lin YW, et al. Regulation of retinal hemodynamics in diabetic rats by increased expression and action of endothelin-1. *Invest Ophthalmol Vis Sci.* 1996;37:2504–2518.

3. Chakravarthy U, Hayes RG, Stitt AW, Douglas A. Endothelin expression in ocular tissues of diabetic and insulin-treated rats. *Invest Ophthalmol Vis Sci.* 1997;38:2144–2151.

4. Takagi C, King GL, Takagi H, Lin YW, Clermont AC, Bursell SE. Endothelin-1 action via endothelin receptors is a primary mechanism modulating retinal circulatory response to hyperoxia. *Invest Ophthalmol Vis Sci.* 1996;37:2099–2109.

5. Trick GL, Berkowitz BA. Retinal oxygenation response and retinopathy. *Prog Retin Eye Res.* 2005;24:259–274.

6. Yu DY, Cringle SJ, Alder V, Su EN. Intraretinal oxygen distribution in the rat with graded systemic hyperoxia and hypercapnia. *Invest Ophthalmol Vis Sci.* 1999;40:2082–2087.

7. Pournaras JA, Petropoulos IK, Munoz JL, Pournaras CJ. Experimental retinal vein occlusion: effect of acetazolamide and carbogen (95% O_2/5% CO_2) on preretinal PO_2. *Invest Ophthalmol Vis Sci.* 2004;45:3669–3677.

8. Kowluru RA, Engerman RL, Kern TS. Abnormalities of retinal metabolism in diabetes or experimental galactosemia VIII: prevention by aminoguanidine. *Curr Eye Res.* 2000;21:814–819.

9. Berkowitz BA, Ito Y, Kern TS, McDonald C, Hawkins R. Correction of early subnormal superior hemiretinal DeltaPO(2) predicts therapeutic efficacy in experimental diabetic retinopathy. *Invest Ophthalmol Vis Sci.* 2001;42:2964–2969.

10. Park JY, Takahara N, Gabriele A, et al. Induction of endothelin-1 expression by glucose: an effect of protein kinase C activation. *Diabetes.* 2000;49:1239–1248.

11. Berkowitz BA, Luan H, Gupta RR, et al. Regulation of the early subnormal retinal oxygenation response in experimental diabetes by inducible nitric oxide synthase. *Diabetes.* 2004;53:173–178.

12. Clozel M, Breu V, Gray GA, et al. Pharmacological characterization of bosentan, a new potent orally active nonpeptide endothelin receptor antagonist. *J Pharmacol Exp Ther.* 1994;270:228–235.

13. Cosenzi A, Bernobich E, Plazzotta N, Seculin P, Bellini G. Bosentan reduces blood pressure and the target-organ damage induced by a high-fructose diet in rats. *J Hypertens.* 1999;17:1843–1848.

14. Ding SS, Qiu C, Hess P, Xi JF, Zheng N, Clozel M. Chronic endothelin receptor blockade prevents both early hyperfiltration and late overt diabetic nephropathy in the rat. *J Cardiovasc Pharmacol.* 2003;42:48–54.

15. Arikawa E, Verma S, Dumont AS, McNeill JH. Chronic bosentan treatment improves renal artery vascular function in diabetes. *J Hypertens.* 2001;19:803–812.

16. Chen S, Khan ZA, Cukiernik M, Chakrabarti S. Differential activation of NF-kappa B and AP-1 in increased fibronectin synthesis in target organs of diabetic complications. *Am J Physiol.* 2003;284:E1089–E1097.

17. Evans T, Deng DX, Chen S, Chakrabarti S. Endothelin receptor blockade prevents augmented extracellular matrix component mRNA expression and capillary basement membrane thickening in the retina of diabetic and galactose-fed rats. *Diabetes.* 2000;49:662–666.

18. Li JS, Knafo L, Turgeon A, Garcia R, Schiffrin EL. Effect of endothelin antagonism on blood pressure and vascular structure in renovascular hypertensive rats. *Am J Physiol.* 1996;271:H88–H93.

19. Berkowitz BA, Zhang W. Significant reduction of the panretinal oxygenation response after 28% supplemental oxygen recovery in experimental ROP. *Invest Ophthalmol Vis Sci.* 2000;41:1925–1931.

20. Lutty GA, McLeod DS. A new technique for visualization of the human retinal vasculature. *Arch Ophthalmol.* 1992;110:267–276.

21. Brain SD. The direct observation of arteriolar constriction induced by endothelin in vivo. *Eur J Pharmacol.* 1989;160:401–403.

22. Bursell SE, Clermont AC, Oren B, King GL. The in vivo effect of endothelins on retinal circulation in nondiabetic and diabetic rats. *Invest Ophthalmol Vis Sci.* 1995;36:596–607.

23. Berkowitz BA. Adult and newborn rat inner retinal oxygenation during carbogen and 100% oxygen breathing: comparison using magnetic resonance imaging delta P_{O_2} mapping. *Invest Ophthalmol Vis Sci.* 1996;37:2089–2098.

24. Berkowitz BA. Role of dissolved plasma oxygen in hyperoxia-induced contrast. *Magn Reson Imag.* 1997;15:123–126.

25. Berkowitz BA. The role of dissolved plasma oxygen in hyperoxia induced contrast. *Magn Reson Imaging.* 1995;15:123–126.

26. Tofts PS, Berkowitz BA. Rapid measurement of capillary permeability using the early part of the dynamic Gd-DTPA MRI enhancement curve. *J Magn Reson.* 1993;102:129–136.

27. Ettl A, Fischer-Klein C, Chemelli A, Daxer A, Felber S. Proton relaxation times of the vitreous body in hereditary vitreoretinal dystrophy. *Ophthalmologica.* 1994;208:195–197.

28. Hopkins AL, Yeung HN, Bratton CB. Multiple field strength in vivo T1 and T2 for cerebrospinal fluid protons. *Magn Reson Med.* 1986;3:303–311.

29. Luoma K, Raininko R, Nummi P, Luukkonen R. Is the signal intensity of cerebrospinal fluid constant?—intensity measurements with high and low field magnetic resonance imagers. *Magn Reson Imaging.* 1993;11:549–555.

30. Meyer ME, Yu O, Eclancher B, Grucker D, Chambron J. NMR relaxation rates and blood oxygenation level. *Magn Reson Med.* 1995;34:234–241.

31. Alder VA, Yu DY, Cringle SJ. Vitreal oxygen tension measurements in the rat eye. *Exp Eye Res.* 1991;52:293–299.

32. Liang Z. Longitudinal data analysis using generalized linear models. *Biometrika.* 1986;73:13–22.

33. Chakrabarti S, Cukiernik M, Hileeto D, Evans T, Chen S. Role of vasoactive factors in the pathogenesis of early changes in diabetic retinopathy. *Diabetes Metab Res Rev.* 2000;16:393–407.

34. Evans T, Xi DD, Mukherjee K, Downey D, Chakrabarti S. Endothelins, their receptors, and retinal vascular dysfunction in galactose-fed rats. *Diabetes Res Clin Pract.* 2000;48:75–85.

35. Ahmed J, Pulfer MK, Linsenmeier RA. Measurement of blood flow through the retinal circulation of the cat during normoxia and hypoxemia using fluorescent microspheres. *Microvasc Res.* 2001;62:143–153.

36. Linsenmeier RA, Braun RD. Oxygen distribution and consumption in the cat retina during normoxia and hypoxemia. *J Gen Physiol.* 1992;99:177–197.

37. Yamamoto F, Steinberg RH. Effects of systemic hypoxia on pH outside rod photoreceptors in the cat retina. *Exp Eye Res.* 1992;54:699–709.

38. Berkowitz BA, Roberts R, Luan H, et al. Drug intervention can correct subnormal retinal oxygenation response in experimental diabetic retinopathy. *Invest Ophthalmol Vis Sci.* 2005;46:2954–2960.

39. Schmetterer L, Wolzt M. Ocular blood flow and associated functional deviations in diabetic retinopathy. *Diabetologia.* 1999;42:387–405.